

the desired substrate adjacent to a catalytic subsite and thereby accelerate the desired reaction, then he or she can essentially achieve what nature has achieved through natural enzymes.

Authors are grateful to Dr. R. C. Gadwood of the Upjohn Co. for the help with the CHEMGRAF computer structures. This work

was financially aided by the National Institute of Health (Grant GM-20853), the National Science Foundation (Grant CHE-802697), Merck Sharp and Dohme Co., Hoffman-La Roche Co., Dow Chemical Co. Fdn., and Monsanto Chemical Co. It is now being supported by the Office of Naval Research. This support is gratefully acknowledged. Finally, the inspiration for these advances can be attributed to Dr. F. H. Westheimer.

## Carbon-13 Shielding Tensors: Experimental and Theoretical Determination

JULIO C. FACELLI, DAVID M. GRANT,\* and JOSEF MICHL†

Department of Chemistry, University of Utah, Salt Lake City, Utah 84112

Received October 9, 1986 (Revised Manuscript Received January 27, 1987)

### I. Introduction

With the formulation of rules for substituent effects<sup>1-3</sup> in the mid-1960s, <sup>13</sup>C NMR spectroscopy became one of the premier methods for structural and conformational analysis in organic chemistry.<sup>4</sup> It is not at all uncommon for practicing chemists to monitor chemical processes using both <sup>1</sup>H and <sup>13</sup>C NMR spectral methods, as even subtle structural changes correlate nicely with variations in the isotropic chemical shift. The high sensitivity of such liquid data upon chemical structure has been very well documented during the past two decades, and extensive cataloging of trends and spectral features is now available for essentially all classes of organic chemicals.

The complete chemical shielding interaction, however, is given by a tensor which depends upon the electronic structure of the molecule and can be used to describe how the NMR resonance frequency changes with the molecular orientation in the external magnetic field. In nonviscous liquids only the average of the principal values of the tensor, i.e., the isotropic liquid shift, is observed due to the averaging from the rapid rotational motion.

Julio C. Facelli was born in Buenos Aires in 1953. He attended the University of Buenos Aires where he obtained his Licenciado degree in 1977 and his Doctoral degree in Physics in 1981. He has worked as a postdoctoral associate at the University of Arizona and the University of Utah, where currently he is an Assistant Research Professor. His research interests are centered in computational applications to chemistry, with strong interests in solid-state NMR and theoretical calculations of NMR parameters.

David M. Grant has worked in the area of nuclear magnetic resonance since his Ph.D. in 1957. After completing a postdoctoral year at the University of Illinois where he was closely associated with both H. S. Gutowsky and M. Karplus, he has been on the faculty at the University of Utah. His present interest in <sup>13</sup>C shielding tensors culminates almost three decades of interest in <sup>13</sup>C NMR methods as they relate to molecular structure and dynamics.

Josef Michl was born in 1939 in Prague, Czechoslovakia, where he obtained his M.S. degree from Charles University with V. Horák and P. Zuman and his Ph.D. degree from the Czechoslovak Academy of Sciences with R. Zahradník. After postdoctoral years with R. S. Becker at the University of Houston and M. J. S. Dewar at the University of Texas and a brief stay with A. C. Albrecht at Cornell University, he was a staff scientist at the Academy of Sciences in Prague. He left Czechoslovakia in 1968 and spent postdoctoral years with J. Linderberg at Aarhus University, Denmark, and with F. E. Harris at the University of Utah, where he subsequently joined the faculty. In 1986, he moved from Utah to the University of Texas at Austin, where he holds the Marvin K. Collie-Welch Regents Chair in Chemistry. Since 1984, he has been the editor of *Chemical Reviews*. His primary interest is physical organic chemistry.

These tensorial shifts with three principal values have the potential to reveal up to 3 times the information of isotropic shifts, and it is possible from these principal values to obtain "three-dimensional" information on molecular structure and the associated electronic features. Section II outlines in more detail the nature and importance of shielding tensors.

Except for limited, early pioneering work,<sup>5-7</sup> the measurement of <sup>13</sup>C shielding tensors for more than a few molecules has been left until recently. Due to the previous lack of a comprehensive body of experimental data as well as to earlier inadequacies of theoretical methods for systematizing the structural variations, correlations between measured shielding tensorial components and chemical structure are only now emerging. This relative lack of research in the area of <sup>13</sup>C shielding tensors, in spite of their clear advantages, results in part from the difficulty of solid-state NMR techniques compared with standard isotropic liquid work.

The measurement of <sup>13</sup>C shielding tensors involves the analysis of single-crystal rotation data or line shape analysis of powder samples where small crystallites orient in all possible directions. Use is made of the cross-polarization method to enhance the sensitivity with high-power <sup>1</sup>H decoupling to eliminate the <sup>1</sup>H-<sup>13</sup>C dipolar interactions. A detailed description of the experimental techniques is given in section III.

The principal tensorial shielding values can be obtained from spectral patterns obtained on powdered solids, providing tensorial patterns from nonequivalent nuclei are not so severely overlapping as to obscure break points (cusps and shoulders) and other spectral

† Present address: Department of Chemistry, University of Texas, Austin, TX 78712-1167.

(1) Grant, D. M.; Paul, E. G. *J. Am. Chem. Soc.* 1964, 86, 2984.  
 (2) Grant, D. M. In *Magnetic Resonance*; Coogan, C. K., Norman, S. H., Stuart, S. N., Pilbrow, J. R., Wilson, G. V. H., Eds.; Plenum: New York, 1970; p 323. Abstract also printed in: *Vortex* 1970, 65, 27.  
 (3) Grant, D. M. *Pure Appl. Chem.* 1974, 37, 61.  
 (4) Levy, G. L.; Nelson, G. C. *Carbon-13 Nuclear Magnetic Resonance for Organic Chemists*; Wiley-Interscience: New York, 1972.  
 (5) Pausak, A.; Pines, A.; Waugh, J. S. *J. Chem. Phys.* 1973, 59, 591.  
 (6) Chang, J. J.; Griffin, R. G.; Pines, A. *J. Chem. Phys.* 1974, 60, 2561.  
 (7) Mahnke, H.; Sheline, R. K.; Spiess, H. W. *J. Chem. Phys.* 1974, 61, 55.

details upon which the curve fitting and data reduction depend. Usually such simple spectra presume molecules which are usually liquids or gases at room temperature. These considerations led us to introduce low-temperature NMR techniques in 1978, which allow the recording of spectra of either substances in the form of neat solids or molecules trapped and isolated in inert gas matrices.<sup>8,9</sup>

Use of single-crystal spectroscopic techniques provides a superior method for obtaining both principal tensorial values as well as the orientation of the corresponding principal axes, but unfortunately single-crystal methods suffer from the difficulties associated with growing crystals, which must be larger (50 mm<sup>3</sup> or more) than those typically used for X-ray structural analysis, and from the need for extensive methods of data reduction.

The interpretation and cataloging of experimentally measured <sup>13</sup>C shielding tensors require "state of the art" quantum chemical calculations, which only recently have developed with an accuracy sufficient to correlate measured tensors with electronic structural features. These calculations become even more critical in the case of powder patterns where only the principal values of the tensor can be measured. Theory is left with the task of identifying the orientation of the tensor's principal axes in the molecular frame.

In this Account the origin and experimental manifestation of the chemical shielding tensor are summarized, followed by a discussion of the different experimental techniques for measuring <sup>13</sup>C shielding tensors. Emphasis is placed on the low-temperature technique introduced in this laboratory<sup>8,9</sup> because it has provided the largest body of data to date, but references are given to other techniques (single-crystal and liquid-crystal work) commonly used to obtain <sup>13</sup>C shielding anisotropies and tensors. The theoretical section includes a brief review of different methods for calculating shielding tensors. The basic ideas of the IGLO<sup>10</sup> (individual gauge for localized orbitals) bond contribution analysis in the local bond frame<sup>11</sup> are presented, as this method nicely parallels traditional chemical concepts. Finally, several representative examples of <sup>13</sup>C shielding tensors and their relationships with molecular structure are presented. In the conclusion, the future goals and the potential of this spectroscopic technique as a practical tool in the elucidation of molecular structure are discussed briefly.

## II. Shielding Tensors

The chemical shielding of a magnetic nucleus originates in the electronic cloud that surrounds the nuclei in a molecule. In contrast with an atom, the electronic cloud in even the simplest molecule is not spherically symmetric due to chemical bonding. Thus, the electronic shielding of the nucleus has been found to depend on the molecular orientation with respect to the external magnetic field. The appropriate mathematical formulation to describe this physical property is a tensor,<sup>12</sup> and the interaction between the external

magnetic field,  $\vec{H}$ , and the nuclear magnetic moment,  $\vec{I}$ , is given by the following Hamiltonian

$$\mathcal{H} = \vec{H} \cdot (\vec{1} - \vec{\sigma}) \cdot \vec{I} \quad (1)$$

where  $\vec{\sigma}$  is the Cartesian representation of the shielding tensor and  $\vec{1}$  is the unit tensor. It often surprises new workers in the field to find that  $\vec{\sigma}$  is not a symmetric tensor. However, only the symmetric components of the tensor contribute to first order in the external magnetic field (10–1000 ppm) to the normal NMR spectra.<sup>13–15</sup> The antisymmetric components contribute to second order in the magnetic field, producing negligible effects on spectra at achievable fields; they also contribute to the spin relaxation mechanisms.<sup>16</sup> Details concerning the symmetry properties of the  $\vec{\sigma}$  tensors abound in the literature<sup>17–19</sup> and are not reproduced here.

The spectrum associated with the Hamiltonian in eq 1 for a single nucleus at a fixed orientation will be a single line whose position depends on the relative orientation of the magnetic field  $\vec{H}$  in the molecular frame. A typical spectrum of a single crystal is the superposition of the lines arising from all the nonequivalent nuclei in the crystallographic unit cell. Whenever dipolar interactions between magnetic nuclei are present, the spectra also will show the characteristic splittings by the dipolar interactions.<sup>13,20</sup> Samples with dilute spin species like <sup>13</sup>C do not encounter such splittings, providing some method is used to decouple the dipolar interactions with abundant spins (usually protons) in the sample.

If the molecules in the sample do not exhibit the highly ordered characteristic of a single crystal (e.g., a sample which is a genuine amorphous solid or a collection of randomly oriented microcrystals), then the spectra will be given by the ensemble average of the Hamiltonian (1) over all possible molecular orientations and chemical environments. The calculation of these powder patterns has been discussed in the literature,<sup>13,20</sup> eliminating the need to provide the mathematical details here. For illustration purposes Figure 1 contains powder patterns arising from two simple shielding tensors. The cases shown are for carbon dioxide, which has an axially symmetric tensor with two degenerate principal values, and for ethylene with an asymmetric tensor where all three principal values are different. It is not necessary to show the spherically symmetric case with three degenerate principal values, as it yields a single resonance line with a resonance frequency that is independent of the relative orientation of the magnetic field within the molecular framework.

Of the two examples shown in Figure 1, only the axially symmetric case provides principal values, which

(12) Rose, M. E. *Elementary Theory of Angular Momentum*; Wiley: New York, 1967.

(13) Haeberlen, U. *High Resolution NMR in Solids, Selective Averaging Advances in Magnetic Resonance*; Academic: New York, 1976; Suppl. 1.

(14) Schneider, R. F. *J. Chem. Phys.* 1968, 48, 4905.

(15) Griffin, R. G.; Ellet, J. D.; Mehring, M.; Bullitt, J. G.; Waugh, J. S. *J. Chem. Phys.* 1972, 57, 2147.

(16) Spiess, H. W. *NMR: Basic Princ. Prog.* 1978, 15, 59.

(17) Facelli, J. C.; Orendt, A. M.; Grant, D. M.; Michl, J. *J. Chem. Phys. Lett.* 1984, 112, 147.

(18) Buckingham, A. D.; Malm, S. M. *Mol. Phys.* 1971, 22, 1127.

(19) Robert, J. B.; Wiesenfeld, L. *Phys. Rep.* 1982, 86, 363.

(20) Mehring, M. *NMR: Basic Princ. Prog.* 1976, 11, 1.

(8) Zilm, K. W.; Conlin, R. T.; Grant, D. M.; Michl, J. *J. Am. Chem. Soc.* 1978, 100, 8038.

(9) Zilm, K. W.; Conlin, R. T.; Grant, D. M.; Michl, J. *J. Am. Chem. Soc.* 1980, 102, 6672.

(10) Kutzelnigg, W. *Isr. J. Chem.* 1980, 19, 193.

(11) Facelli, J. C.; Grant, D. M.; Michl, J. *Int. J. Quantum Chem.*, in press.

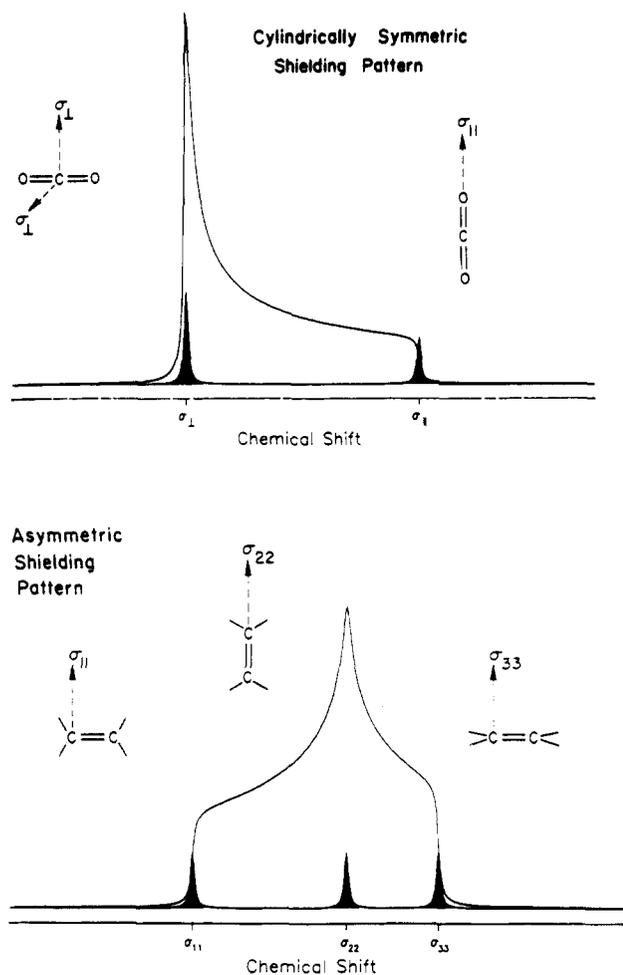


**Figure 1.** Powder patterns for a nonaxially symmetric tensor (top) and for an axially symmetric tensor (bottom). The position of the principal values is indicated in the spectra.

can be assigned to the principal axes of the shielding tensor by using the symmetry rules of Buckingham and Malm.<sup>18</sup> In cases of lower symmetry the orientation of one or more of the principal axes of the shielding tensor may be known from symmetry considerations,<sup>18</sup> but there is no experimental way to assign the principal values obtained from a powder pattern to the three principal axes (i.e., there are six possible permutations for assigning three measured principal values to three principal axes). In the absence of any symmetry or in very low symmetry cases, information is unavailable for even specifying the orientation of the principal shielding axes in the molecular frame. Some information can be obtained from dipolar spectroscopy<sup>21</sup> or certain two-dimensional techniques,<sup>22,23</sup> but their use is by no means general nor is the interpretation of the spectra simple.

In the absence of experimental data on the orientation of the principal axes of the shielding tensor in the molecular frame, theoretical calculations provide the only way for designating the orientation of principal axes and assigning to them the principal values. The use of theory for making these tentative assignments is supported by the good agreement between the measured and calculated principal values and the corresponding orientation of the principal axes in molecules

where symmetry or independent information exists for making unequivocal assignments.<sup>24-28</sup>

Two main sources of measured <sup>13</sup>C shielding tensors exist in the literature: the review by Veeman<sup>29</sup> on <sup>13</sup>C shielding tensors measured by solid-state NMR techniques and the review by Lounila and Jokisaari<sup>30</sup> for data obtained in solutions of liquid crystals.

### III. Experimental Techniques

Rapidly reorienting molecules prevent the direct measurement of <sup>13</sup>C shielding tensors whenever this motion is random with respect to the external magnetic field and faster than the NMR time scale. Under these conditions, the tensorial spectral response is averaged to the isotropic shift given by the tensor's trace and the anisotropic data are lost. Thus, tensor measurements require either some degree of preferential ordering in dynamically tumbling samples or else a static solid sample in either powder or single-crystal form. The former method has been used for molecules dissolved in liquid crystals and has been reviewed recently.<sup>30</sup> Unfortunately, the results in liquid crystals are severely limited by uncertainties in the order parameters and by solvent-induced chemical shifts. Several interesting advances in this area, however, have been reported recently by Fung.<sup>31</sup>

A more reliable and common method to measure <sup>13</sup>C shielding interactions involves the use of static samples, with the single-crystal approach preferable to powder methods for obtaining the greatest amount of information on the shielding tensors. The single-crystal method, however, is generally not easily applicable to samples which are liquids or gases at room temperature where low temperature is required to solidify the sample. Even molecules that are solid at room temperature may exhibit fast rotational modes in the solid phase that preclude the complete measurement of the shielding tensors. Low-temperature methods for neat powders and for molecules deposited in inert gas matrices provide a relatively rapid and convenient way to obtain powder patterns on small molecules. The use of powders suffers from two main limitations. First, only the principal values are obtainable from the spectra,<sup>13,20</sup> and information on the orientation of the axes either is unavailable or depends on symmetry arguments. Second, overlapping tensorial patterns may become too complicated to extract the tensorial information if more than one nonequivalent carbon is present per molecule. In spite of these difficulties, computational techniques have been developed in this laboratory to overcome the problem of several (up to three or four nuclei) overlapping powder patterns.<sup>32</sup> An

(24) Beeler, A. J.; Orendt, A. M.; Grant, D. M.; Cutts, P. W.; Michl, J.; Zilm, K. W.; Downing, J. W.; Facelli, J. C.; Schindler, M. S.; Kutzelnigg, W. *J. Am. Chem. Soc.* **1984**, *106*, 7672.

(25) Facelli, J. C.; Orendt, A. M.; Beeler, A. J.; Solum, M. S.; Grant, D. M.; Michl, J.; Depke, G.; Malsch, K. D.; Murthy, P. *J. Am. Chem. Soc.* **1985**, *107*, 6749.

(26) Orendt, A. M.; Facelli, J. C.; Grant, D. M.; Michl, J.; Walker, F. H.; Dailey, W. P.; Waddell, S. T.; Wiberg, K. B.; Schindler, M.; Kutzelnigg, W. *Theor. Chim. Acta* **1985**, *68*, 421.

(27) Facelli, J. C.; Orendt, A. M.; Solum, M. S.; Depke, G.; Grant, D. M. *J. Am. Chem. Soc.* **1986**, *108*, 4268.

(28) Solum, M. S.; Facelli, J. C.; Michl, J.; Grant, D. M. *J. Am. Chem. Soc.* **1986**, *108*, 6464.

(29) Veeman, W. S. *Prog. Nucl. Magn. Reson. Spectrosc.* **1984**, *16*, 193.

(30) Lounila, J.; Jokisaari, J. *Prog. Nucl. Magn. Reson. Spectrosc.* **1982**, *15*, 249.

(31) Parhami, P.; Fung, B. M. *J. Am. Chem. Soc.* **1985**, *107*, 7304.

(21) Zilm, K. W.; Grant, D. M. *J. Am. Chem. Soc.* **1981**, *103*, 2913.

(22) Stoll, M. E.; Vega, A. J.; Vaughan, R. W. *J. Chem. Phys.* **1976**, *65*, 4093.

(23) Linder, M.; Hohener, A.; Ernst, R. R. *J. Chem. Phys.* **1980**, *73*, 4959.

obvious but laborious solution in the study of molecules with many nonequivalent nuclei is to resort to selective <sup>13</sup>C enrichment.

At Utah, we have chosen to use a room-temperature probe with a coil sufficiently large to allow the use of normal low-temperature matrix techniques.<sup>33</sup> Either a Displex or a Helitran (Air Products) cryogenic apparatus is used to cool the sample.<sup>9,34</sup> In the case of stable compounds the deposition of the material, either neat or as a mixture with inert gases (e.g., Ar, Ne) or more reactive gases (e.g., NH<sub>3</sub>, SO<sub>2</sub>), has been found to work successfully for all types of molecules. In the case of reactive compounds greater care is needed in the deposition.<sup>34,35</sup> Other workers<sup>36,37</sup> have cooled the sample along with the NMR probe to very low temperatures with some attendant challenges. In Prof. Waugh's recent efforts<sup>38</sup> the cryogenic apparatus is so massive that it is the magnet which is moved to a position around the NMR probe operating at fractions of a degree kelvin.

The cryogenic apparatus in this laboratory<sup>9,34</sup> is used with a home-built spectrometer<sup>39</sup> described previously. This spectrometer ( $\nu_H = 80$  MHz) uses a special wide-gap (2.25 in.) Varian electromagnet and is controlled with a PDP 11/34 computer. With the current probe, a coil of 12 mm is used to give a Hartmann-Hahn proton matching field of 40 KHz. Typically, the experiments require samples with  $\sim 10^{20}$  <sup>13</sup>C nuclei, cross-polarization times of  $\sim 3$  ms, and a recycle time of several seconds. All these spectral conditions are achievable with commercial solid-state NMR spectrometers. A special, but relatively simple, probe is required to receive the cryogenic apparatus. If superconducting magnet systems are to be used, mechanical considerations would seem to favor the use of a horizontal bore magnet for this type of experiment over the more common vertical magnets.

Use of inert gas matrices also provides an attractive method for study of reactive species which may require isolation in order to preserve their chemical integrity. An application of the technique to reactive species has been published;<sup>35</sup> this use of the NMR matrix method remains largely unexploited to date, but it portends great promise in the future. Currently in progress in our laboratory is the application of such techniques to reactive species which are most conveniently accessible by photolysis of their precursors in an inert gas matrix.

Single-crystal studies require relative large crystals due to the ever present sensitivity limitations of NMR methods. As each unique carbon in the unit cell of a single crystal gives a single, relatively narrow line, the problems of overlapping lines are minimized, though at times not totally eliminated. The systematic rotation of the crystal, with respect to the external magnetic

field, produces rotational patterns which can be computer analyzed to obtain the tensorial principal values and the orientation of the corresponding principal axes.<sup>13</sup> Fitting these rotational patterns leads to shielding information in the bulk crystal frame. In order to obtain the shielding tensor in the molecular frame, it becomes necessary to transform from the laboratory frame into the crystallographic axes and then into the molecular frame. While the second transformation can be obtained from an X-ray structure, the first one may require the determination of the crystallographic axes with respect to the macroscopic axes of the actual crystal used in the NMR experiment. Details of this technique are given elsewhere.<sup>13,29</sup> Following closely positioned lines through these rotational plots can at times introduce ambiguities in the line assignment for crystals with a large number of carbons. A two-dimensional NMR technique has been proposed to overcome these problems<sup>40</sup> by correlating spectral responses with a rotational displacement large enough to remove the ambiguity. Such a large-angle flipping technique has the potential for greatly reducing the labor associated with single-crystal studies and is therefore receiving attention in this laboratory.

#### IV. Theoretical Methods

The theory of chemical shielding was reviewed a few years ago by Ebraheem and Webb,<sup>41</sup> and thereafter the progress in the field has been reported by Jameson.<sup>42</sup> This section will not give a comprehensive review of shielding theory but will describe briefly the present "state of the art" and the role that theoretical calculations can play in the analysis of shielding tensors.

It is well documented<sup>43-45</sup> that good results can be obtained in the calculation of <sup>13</sup>C chemical shieldings using the coupled Hartree-Fock (CHF)<sup>46</sup> theory, providing sufficiently extensive basis sets are used. Unfortunately, these calculations are limited to small or highly symmetrical molecules because of the large basis sets required in the CHF calculations to assure the proper gauge invariance of the results.<sup>47</sup> To overcome these problems, two basic approaches have been used: (a) the GIAO (gauge invariance atomic orbitals) method of Ditchfield<sup>48</sup> and (b) the IGLO (individual gauge for localized orbitals) approach of Kutzelnigg.<sup>10</sup> Recently, the LORG (localized orbital/local origin) method, essentially equivalent to the IGLO method, has been proposed by Hansen and Bouman.<sup>49</sup> The LORG method uses the first-order polarization propagator approach (FOPPA) or random phase approximation (RPA)<sup>50</sup> instead of the equivalent CHF perturbation theory. The GIAO methods can produce reasonable results<sup>51</sup> with a relative small basis set, but the inter-

(32) Alderman, D. W.; Solum, M. S.; Grant, D. M. *J. Chem. Phys.* **1986**, *84*, 3717.

(33) Craddock, S.; Hinchcliff, A. J. *Matrix Isolation: A Technique for Study of Reactive Inorganic Species*; Cambridge University Press: Cambridge, 1975.

(34) Beeler, A. Ph.D. Thesis, University of Utah, 1984.

(35) Strub, H.; Beeler, A. J.; Grant, D. M.; Michl, J.; Cutts, P. W.; Zilm, K. W. *J. Am. Chem. Soc.* **1983**, *105*, 3333.

(36) Matsui, T.; Terao, T.; Saika, A. *J. Chem. Phys.* **1982**, *77*, 1788.

(37) Linder, M.; Höhener, A.; Ernst, R. R. *J. Magn. Reson.* **1979**, *35*, 379.

(38) Weil, J. L.; Tan, S. L.; Waugh, J. S.; Osheroff, D. D. *J. Magn. Reson.* **1986**, *66*, 264.

(39) Solum, M. S. Ph.D. Thesis, University of Utah, 1986.

(40) Carter, C. M.; Alderman, D. W.; Grant, D. M. *J. Magn. Reson.* **1985**, *65*, 183.

(41) Ebraheem, K. A. K.; Webb, G. A. *Prog. Nucl. Magn. Reson. Spectrosc.* **1977**, *11*, 149.

(42) Jameson, C. J. In *Specialist Periodical Reports on NMR Spectroscopy*; Webb, G. A., Ed.; The Chemical Society: London, 1985.

(43) Lazzeretti, P.; Rossi, E.; Zanasi, R. *J. Am. Chem. Soc.* **1983**, *105*, 12.

(44) Lazzeretti, P.; Zanasi, R. *J. Chem. Phys.* **1981**, *75*, 5019.

(45) Höller, R.; Lischka, M. *Mol. Phys.* **1980**, *41*, 1017.

(46) Nakatsuji, H. *J. Chem. Phys.* **1974**, *61*, 3728.

(47) Epstein, S. T. *Isr. J. Chem.* **1985**, *22*, 5035.

(48) Ditchfield, R. *Mol. Phys.* **1974**, *27*, 789.

(49) Hansen, A. E.; Bouman, T. D. *J. Chem. Phys.* **1985**, *82*, 5035.

(50) Jorgensen, P.; Simons, J. *Second Quantization—Based Methods in Quantum Chemistry*; Academic: New York, 1981.

pretation of the results in terms of simple molecular quantities encounters a complexity due to the manner in which gauge has been incorporated into the atomic orbitals.<sup>47</sup> The quality of results of the IGLO and LORG methods<sup>49,52-54</sup> is similar to that of the GIAO methods,<sup>51</sup> but the interpretation of the results in terms of bond contributions provides useful insights which can be very appealing to the chemist.<sup>11</sup>

While a total understanding of the shielding mechanisms requires additional work, preliminary results indicate that some intuitive chemical concepts are useful in the visualization of shielding. Within the IGLO theory of chemical shielding,<sup>10</sup> the shielding tensor  $\bar{\sigma}$  for a nucleus with magnetic moment  $\bar{\mu}$  at a position  $\bar{p}$  is given by

$$\bar{\sigma} = 2 \sum_{k=0}^{\text{occ}} \{ \langle \psi_{k0} | \bar{h}_{k2} | \psi_{k0} \rangle - 2 \langle \psi_{k0} | \bar{h}_{k1} | \psi_{k1} \rangle \} \quad (2)$$

where it is possible to define the diamagnetic and paramagnetic IGLO bond contributions by

$$\bar{\sigma}_d^{XY} = \langle \psi_{(X-Y)_0} | \bar{h}_{k2} | \psi_{(X-Y)_0} \rangle \quad (3)$$

$$\bar{\sigma}_p^{XY} = \langle \psi_{(X-Y)_0} | \bar{h}_{k1} | \psi_{(X-Y)_1} \rangle \quad (4)$$

The notation of ref 10 and 11 is followed here.

Due to the tensorial character of eq 2, all the bond contributions must be expressed in a common molecular frame to obtain the total shielding tensor, but the individual bond contributions can be analyzed by rotating them into separate local bond frames.<sup>11</sup> The analysis in the local bond frame allows a better understanding of the intrinsic electronic features that affect the shielding. It is noted that bond contributions in the local bond frames become independent of the explicit molecular geometry, making a comparison in a series of molecules possible.<sup>11,28</sup> This analysis has been used to analyze the <sup>13</sup>C shielding tensors in methine and methyl carbons.<sup>27,28</sup>

Semiempirical theories of chemical shielding are in general less successful than ab initio ones,<sup>41</sup> but their simplicity and low computational cost make them appropriate for larger molecular systems for which current computational resources preclude the use of ab initio methods. In connection with the experimental work done in Utah, the very simple Pople model,<sup>55,56</sup> using an MNDO wave function,<sup>57</sup> has been used to rationalize the in-plane components of the <sup>13</sup>C shielding tensors in pyrene.<sup>58</sup>

### V. Three-Dimensional Information Contained in Tensorial Data

In this section some examples from our laboratory are given to illustrate the information which can be obtained from the techniques discussed above. The examples were selected to show how geometrical and electronic changes are manifest directly in the components of <sup>13</sup>C shielding tensors.

(51) Chestnut, D. B.; Foley, C. K. *Chem. Phys. Lett.* **1985**, *118*, 316.

(52) Schindler, M.; Kutzelnigg, W. *J. Am. Chem. Soc.* **1983**, *105*, 1360.

(53) Schindler, M.; Kutzelnigg, W. *J. Chem. Phys.* **1982**, *76*, 1919.

(54) Schindler, M.; Kutzelnigg, W. *Mol. Phys.* **1983**, *48*, 781.

(55) Pople, J. A. *J. Chem. Phys.* **1962**, *37*, 53.

(56) Pople, J. A. *J. Chem. Phys.* **1962**, *37*, 60.

(57) Dewar, M. J. S.; Thiel, W. *J. Am. Chem. Soc.* **1977**, *99*, 4899.

(58) Carter, C. M.; Alderman, D. W.; Facelli, J. C.; Grant, D. M. *J. Am. Chem. Soc.*, in press.

**Table I.**  
Experimental and Calculated <sup>13</sup>C Shielding Principal Values in Cyclopropane, Cyclobutane, and Cyclopentane<sup>a</sup>

	CCC angle	calculated			experimental
		I <sup>b</sup>	II <sup>b</sup>	III <sup>b</sup>	
cyclopropane	60.0				
σ <sub>AA</sub>		35	38	25	22
σ <sub>BB</sub>		-8	6	6	2
σ <sub>CC</sub>		-15	-39	-40	-36
σ <sub>iso</sub>		4	2	-3	-4 (-2.8) <sup>c</sup>
cyclobutane	88.5				
σ <sub>AA</sub>		26	27	26	23
σ <sub>BB</sub>		-6	9	9	14
σ <sub>CC</sub>		38	35	39	39
σ <sub>iso</sub>		19	24	25	25 (22.1) <sup>c</sup>
cyclopentane	105.0				
σ <sub>AA</sub>		22	31		21
σ <sub>BB</sub>		4	16		12
σ <sub>CC</sub>		45	49		49
σ <sub>iso</sub>		24	32		27 (25.3) <sup>c</sup>

<sup>a</sup>Shielding values in ppm. Experimental values referenced to TMS.<sup>25</sup> Calculated values referenced to methane. σ<sub>AA</sub> lies in the HCH plane bisecting the HCH angle; σ<sub>BB</sub> lies perpendicular to the HCH plane, and σ<sub>CC</sub> lies perpendicular to the CCC plane. For a detailed discussion of the exact orientations of σ<sub>AA</sub>, σ<sub>BB</sub>, and σ<sub>CC</sub> see ref 25. <sup>b</sup>I: (6,3) basis set. II: (9,5) basis set. III: (9,5 + polarization functions) basis set. <sup>c</sup>Isotropic values measured by liquid NMR.

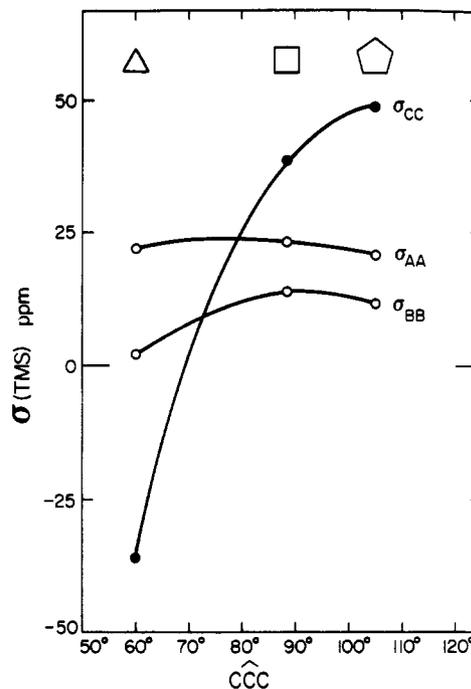


**Figure 2.** <sup>13</sup>C shielding components are shown as a function of the CCC angle in cyclopropane, cyclobutane, and cyclopentane. The orientation of σ<sub>AA</sub>, σ<sub>BB</sub>, and σ<sub>CC</sub> is described in Table I.

**Example 1: Angular Dependence of <sup>13</sup>C Shielding Tensors in Simple Cycloalkanes.** Measured and IGLO<sup>10,53,54</sup> calculated principal values for three simple cycloalkanes (cyclopropane, cyclobutane, and cyclopentane) are presented in Table I. Calculations have been used to sort out and to assign the measured principal values of specific axes in the <sup>13</sup>CH<sub>2</sub> group. The orientations are specified by an effective C<sub>2v</sub> local symmetry with perpendiculars to the two local mirror planes and the third along the local C<sub>2</sub> axis (see Table I for spacial assignments). Without the selection of appropriate permutation of the principal values with the molecular axes, it is impossible to discuss the

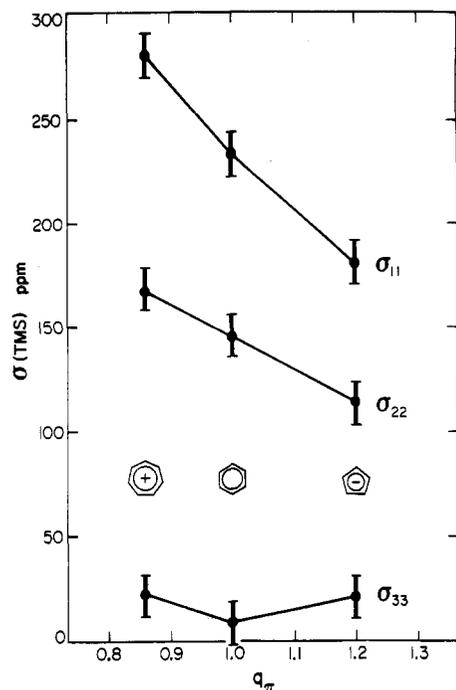


**Figure 3.**  $^{13}\text{C}$  shielding tensor principal components for tropylium cation, benzene, and cyclopentadienide anion as a function of  $\pi$ -electron charge. Experimental values from ref 35. A more extensive line shape analysis<sup>32</sup> has shown that the fitting errors are likely larger than those reported previously. Accordingly, error bars in the current figure have been increased to  $\pm 10$  ppm.

measured principal values in terms of structural features for a given series of compounds. The use of theory to make the spacial assignments is supported by the agreement found between the calculated and measured orientations using double  $^{13}\text{C}$ -labeled material.<sup>25,59</sup>

From the results of Table I, it is apparent that  $\sigma_{AA}$  and  $\sigma_{BB}$  are reasonably constant in all three compounds. Conversely,  $\sigma_{CC}$  moves from  $-36$  ppm in cyclopropane, to  $+39$  ppm in cyclobutane, and on to  $+49$  ppm in cyclopentane. In Figure 2 a correlation between  $\sigma_{CC}$  (with a range of 85 ppm) and the CCC angle is clearly shown. This correlation, supported by theoretical calculations, has been found also for a larger number of compounds, as discussed elsewhere.<sup>25</sup>

As depicted in Table I,  $\sigma_{CC}$  moves from the upfield position in cyclopropane to the downfield position in cyclobutane and cyclopentane. The crossover of  $\sigma_{CC}$  with  $\sigma_{BB}$  is theoretically predicted to occur at about  $70^\circ$ .<sup>25</sup> The high sensitivity, found only in  $\sigma_{CC}$  with changes in the CCC angle, emphasizes the importance of measuring individual tensor components instead of isotropic values. Both  $\sigma_{AA}$  and  $\sigma_{BB}$  fail to exhibit any significant dependence on the CCC angle and partially obscure the true dependence of shielding upon ring size in this homologous series.

**Example 2: The Effect of an Anisotropic  $\pi$ -Electron Charge Distribution on Aromatic Shielding Tensors.** The  $^{13}\text{C}$  shielding dependence upon  $\pi$ -charge,  $q_\pi$ , in aromatic compounds was recognized long ago in the seminal work of Spiess and Schneider.<sup>60,61</sup> In the recent work of this laboratory this relationship of shielding upon  $\pi$ -charge has been

(59) Zilm, K. W.; Beeler, A. J.; Grant, D. M.; Michl, J.; Chou, T. C.; Allred, E. L. *J. Am. Chem. Soc.* **1981**, *103*, 2119.

(60) Spiess, H.; Schneider, W. G. *Tetrahedron Lett.* **1961**, 468.

(61) Fliszar, S.; Cardinal, G.; Beraldin, M. T. *J. Am. Chem. Soc.* **1982**, *104*, 5287.

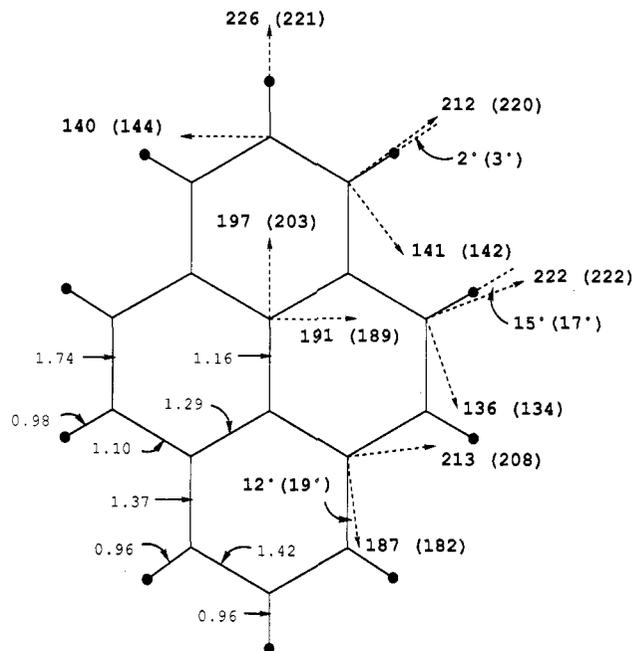


**Figure 4.** Orientation and principal values of in-plane shielding tensors components and calculated bond orders in pyrene. All of the shielding values, given in bold font, are in ppm referenced to TMS with the calculated values given in brackets.

reexamined by using available  $^{13}\text{C}$  tensorial information<sup>35</sup> on  $\text{C}_7\text{H}_7^+$ ,  $\text{C}_6\text{H}_6$ , and  $\text{C}_5\text{H}_5^-$ . The results are summarized in Figure 3, where it is observed that only the two in-plane components ( $\sigma_{11}$  and  $\sigma_{22}$ ) correlate with the nonspherically symmetric  $q_\pi$ . The component  $\sigma_{33}$ , perpendicular to the molecular ring, however, does not have even a monotonic dependence on  $q_\pi$ . This result is not too surprising in view of the aliphatic character of this component, which is influenced primarily by the  $\sigma$ -electrons. The in-plane components ( $\sigma_{11}$  and  $\sigma_{22}$ ) lying along the C-H bond vector and perpendicular to the C-H vector, respectively, are very dependent on the  $\pi$ -electronic charge. Note that the angular momentum along axes in the plane will mix the  $p_\sigma$  orbitals into the antibonding  $\pi^*$  orbital and  $\pi$  orbitals into the antibonding  $p_\sigma^*$  orbitals.<sup>41</sup> These in-plane components are very sensitive to the  $\sigma \rightarrow \pi^*$  and  $\pi \rightarrow \sigma^*$  energy gaps that have been correlated with the  $\pi$ -charge of the molecule.<sup>62</sup> Thus, the charge does not affect the shielding only in a direct isotropic "diamagnetic"-like process, but also through the change of the energy gap between the bonding and antibonding molecular orbitals, which in turn modify the paramagnetic contribution. The change in the charge distribution also affects the magnitude of matrix elements of the  $L$  and  $L/r^3$  operators.<sup>41</sup>

These results are of importance because they clarify the mechanisms by which the chemical shielding is influenced by the anisotropic electronic charge, thereby stressing the importance of tensorial data in characterizing three-dimensional structural features. Such orientationally sensitive data can provide significant insight into the very anisotropic features associated with the  $\pi$ -electron distribution which dominate the chemistry of aromatic systems.

**Example 3: The Use of  $^{13}\text{C}$  Shielding Tensors as a Probe of Aromaticity.** It has been found that ex-

(62) Dewar, M. J. S.; Dougherty, R. C. *The PMO Theory of Organic Chemistry*; Plenum: New York, 1975.

perimental  $^{13}\text{C}$  shielding tensors also can be used as a powerful tool in the analysis of the degree of delocalization of  $\pi$ -electrons in aromatic compounds. The  $^{13}\text{C}$  shielding tensors of aromatic compounds are characterized by two downfield components, below 100 ppm from TMS, and a third component,  $\sigma_{33}$ , between +30 and -30 ppm. This  $\sigma_{33}$  component lies perpendicular to the molecular plane and is mainly determined by the  $\sigma$ -electrons.

The two downfield components lying in the molecular plane, as discussed in example 2, are mainly determined by the  $\pi$ -electron distribution. In Figure 4 the measured and calculated<sup>58</sup> in-plane shielding components in pyrene are given along with the orientation of the principal shielding axes. In addition, the MNDO calculated bond orders<sup>57</sup> are also included.

In spite of the simple model used in the calculations,<sup>58</sup> excellent agreement has been found to exist between the experimental and calculated values. From the results in Figure 4 and related theoretical efforts,<sup>63</sup> it is apparent that a rule emerges on the orientation of the in-plane shielding components in regard to the direction of the  $\pi$ -bonds and degree of localization of these  $\pi$ -electrons as measured by the calculated bond orders. Whenever two of the three bond orders, centered on a  $\text{sp}^2$  carbon, are equal or very nearly equal and differ appreciably from the third bond order,  $\sigma_{11}$  is oriented along or close to the unique bond when this bond has the lowest bond order. If the unique bond order is appreciably greater than the other two equal or near equal bond orders, then  $\sigma_{11}$  orients perpendicular to this unique bond. For the case where all three bonds exhibit different bond orders, the  $\sigma_{11}$  axis strikes a compromise between being parallel to the bond of lowest bond order and perpendicular to the bond of highest bond order. Experimental determination of the orientation of  $\sigma_{11}$  in the  $\text{sp}^2$  plane thus provides a semiquantitative experimental comparison of  $\pi$ -electron bond orders for validation of theoretically calculated bond orders. The relative magnitudes of  $\sigma_{11}$  and  $\sigma_{22}$  also determine the extent of deviation from an axially symmetric distribution of  $\pi$ -electrons about an  $\text{sp}^2$  carbon. It is interesting that such a simple quantum mechanical basis provides an adequate interpretation of the in-plane shielding components in large aromatic compounds. Unfortunately, the method<sup>58,63</sup> is inadequate to provide

satisfactory information on the  $\sigma$ -electrons on which  $\sigma_{33}$  depends. Thus, the third example also documents the importance of both tensorial values and principal axes of orientations as a source of experimentally derived information on three-dimensional electronic structure.

## VI. Conclusions

This Account has attempted to show that the information on chemical structure contained in the individual shielding tensor components is much greater than found in the isotropic shifts, giving detailed information on steric variations, anisotropic charge distributions, bonding to antibonding energy separations, etc.

While the measurement of the shielding tensor is more difficult than for isotropic liquid shifts, it is also clear that the richness of information obtained may at times justify the additional work. Recent results also document that theory is now providing good results that can both assist tensorial assignments and guide the selection of molecules for an experimental program.

Thus, the main goal of the Utah work has been and will continue to be the establishment of a better understanding of relationships existing between chemical and electronic structure of molecules and the individual elements of their shielding tensors. The measurement of shielding tensors is expected to provide a spectroscopic technique for the elucidation of molecular structure, which in many cases will be more powerful than the liquid NMR methods and have the potential for ultimately providing important three-dimensional information on chemical structure.

**Note Added in Proof.** Very recently a variable angle spinning technique has been introduced at Utah. This technique allows the investigation of shielding tensors in powder samples with a large number of nonequivalent shielding tensors.<sup>64</sup>

*The work on shielding tensors at Utah has been mainly supported by the NSF under Grant No. CHE-8310109, but some additional support by the NSF, NIH, and DOE under Grants No. CHE-84-21117, 5 R01 GM 08521-26, and DE-FG02H86ER13510, respectively, is also gratefully acknowledged. We express our gratitude to all our co-workers who made this manuscript possible. We gratefully acknowledge a copy of the IGLO program provided by Drs. W. Kutzelnigg and M. Schindler.*

(63) Facelli, J. C.; Grant, D. M. *Theor. Chim. Acta*, in press.

(64) Sethi, N. K.; Grant, D. M.; Pugmire, R. J. *J. Magn. Reson.*, in press.